



Research article

Tumor cell-derived exosomal miR-193b-3p promotes tumor-associated macrophage activation to facilitate nasopharyngeal cancer cell invasion and radioresistances

Weiwei Li ^{a,b,c,d}, Xing Xing ^{a,b,c,d}, Chunying Shen ^{a,b,c,d}, Chaosu Hu ^{a,b,c,d,*}

^a Department of Radiation Oncology, Fudan University Shanghai Cancer Center, Shanghai, China

^b Department of Oncology, Shanghai Medical College, Fudan University, Shanghai, China

^c Shanghai Clinical Research Center for Radiation Oncology, China

^d Shanghai Key Laboratory of Radiation Oncology, Shanghai, China

ARTICLE INFO

Keywords:

Nasopharyngeal cancer
Tumor-associated macrophages
Exosome
miR-193b
Metastasis

ABSTRACT

Background: Communication between cancer cells and tumor-associated macrophages (TAMs) in the tumor microenvironment (TME) plays a crucial role in accelerating nasopharyngeal cancer (NPC) metastasis and radioresistance. However, the mechanisms through which NPC cells regulate the properties and activation of TAMs during NPC progression are not yet fully understood.

Methods: A high-metastatic NPC subclone (HMC) and a low-metastatic NPC subclone (LMC) were screened from the CNE-2 cell line and exosomes were collected from HMCs and LMCs, respectively. The effects of HMC- and LMC-derived exosomes (HMC-Exos and LMC-Exos) on the regulation of TAM activation were evaluated by assessing the levels of inflammation-related or immunosuppression-related genes. The role of miRNA-193b-3p (miR-193b) in mediating communication between NPCs and TAMs was assessed using real-time quantitative reverse transcription-polymerase chain reaction (qRT-PCR), Western blot analysis, Transwell assays, and clonogenic survival assays.

Results: HMCs and HMC-Exos exhibited a greater capacity to facilitate macrophage protumorigenic activation than LMCs and LMC-Exos. miR-193b levels derived from HMC-Exos were higher than those from LMC-Exos, and miR-193b levels were higher in metastatic NPC tissue-derived TAMs than in non-metastatic NPC tissue-derived TAMs. The upregulated miR-193b was packaged into exosomes and transferred to macrophages. Functionally, miR-193b up-regulation accelerated TAM activation by directly *targeting mitogen-activated protein/ERK kinase kinase 3 (MEKK3)*. As a result, miR-193b-overexpressed macrophages facilitated NPC cell invasion and radioresistance.

Conclusions: These data revealed a critical role for exosomal miR-193b in mediating intercellular communication between NPC cells and macrophages, providing a potential target for NPC treatment.

* Corresponding author. Department of Radiation Oncology, Fudan University Shanghai Cancer Center, Shanghai, 200025, China.
E-mail address: hucusu62@163.com (C. Hu).

1. Introduction

Nasopharyngeal cancer (NPC) is a unique malignancy that originates in the nasopharyngeal epithelium [1] and has a low incidence worldwide, with 133,354 new cases and 80,008 deaths reported in 2020 [2,3]. Several environmental factors (such as Epstein-Barr virus and volatile nitrosamines) are closely correlated with NPC development [3,4]. According to the National Comprehensive Cancer Network guidelines, radiotherapy and concurrent chemoradiotherapy are the standard approaches for patients with early stage and locally advanced NPC, respectively [5]. However, distant metastases and resistance to radiotherapy are major obstacles to the effective treatment of NPC [6].

Macrophages are abundant immune cells in the tumor microenvironment (TME), and tumor-associated macrophages (TAMs) have an immunosuppressive phenotype and accelerates cancer growth, metastasis, and therapy resistance [7–9]. TAM aggregation and activation are frequently associated with poor clinical outcomes in most tumor types [10,11]. In primary tumor tissues, TAM contribute to angiogenesis and cancer cell invasion by inhibiting cytotoxic T cells and natural killer (NK) cell-triggered immune responses [12,13]. In metastatic tumor tissues, TAM promote cancer cell survival, proliferation, and drug (and/or radiation) resistance [11]. Therefore, therapeutic strategies targeting TAM may remodel the immunosuppressive TME by inhibiting TAM activation, polarizing macrophage anti-tumorigenic phenotypes, and accelerating cytotoxic T cell and NK cell activation [14,15].

Communication between cancer cells and macrophages has been widely investigated [16,17]. Wang et al. reported that pancreatic cancer cell-originated exosomes contain a high abundance of microRNA (miR)-301a-3p, and exosomal miR-301a-3p promotes macrophage “M2” polarization to promote pancreatic cancer metastasis [18]. MiR-138-5p can be transferred to TAMs from breast cancer cells through exosomes and promotes macrophage “M2” polarization to advance lung metastasis of breast cancer [19]. However, the mechanism through which NPC cells promote TAM activation remains poorly understood.

Exosomes are lipid double-layered microvesicles with a diameter of 30–100 nm [20]. The biological roles of exosomes depend on their bioactive cargo (lipids, proteins, metabolites, and nucleic acids), which is transferred to recipient cells [21]. Exosomes are generated and secreted by several cell types and play a critical role in intercellular communication to regulate cell viability, the immune response [22], the TME [23], and tumor progression [24]. For example, exosomal miR-34c suppresses NPC progression and alleviates radioresistance in NPC [25]. Highly metastatic hepatocellular carcinoma (HCC) cell-derived exosomal miR-1247-3p can transform normal fibroblasts into tumor-associated fibroblasts to promote tumor metastasis [20]. Because of the important roles of exosomal miRNAs in regulating the TME, which is closely correlated with tumor progression [26–28], we questioned whether exosomal miRNA-mediated communication within the TME is crucial for NPC metastasis and radioresistance. In the present study, we aimed to identify functional miRNAs within NPC cell-derived exosomes and investigate their roles in regulating TAM activation.

2. Materials and methods

2.1. Clinical specimens

Following the approval of the Ethics Committee of Fudan University Shanghai Cancer Center, 17 metastatic and 17 non-metastatic NPC tissues were collected between March 2019 and September 2020 (approval No. 050432-2108*), with informed consent. Peripheral blood samples were collected from 21 patients with NPC. Peripheral blood mononuclear leukocytes (PBMCs) were collected using Ficoll-Hypaque density centrifugation, and CD68⁺ macrophages were purified as blood-derived macrophages (BDMs) using flow cytometry [29,30].

2.2. Data acquisition and analysis

To identify functional miRNAs associated with NPC progression and radiation resistance, the Gene Expression Omnibus (GEO) database (<https://www.ncbi.nlm.nih.gov/gds/>) was used to obtain two datasets (GSE48502 and GSE118720). A series of matrix files was downloaded from the GSE48502 and GSE118720 datasets. After data preprocessing through background correction, data normalization, and principal component analysis, the differentially expressed miRNAs with $|FC| > 1.5$ and $p < 0.05$ were identified. Venn diagram analysis was performed to identify concurrently dysregulated miRNAs in the two datasets.

2.3. Cell culture

The human monocytic cell line U937 was purchased from the American Tissue Culture Collection (ATCC; VA, USA), and cultured in Dulbecco's modified Eagle medium (DMEM; Invitrogen, CA, USA) containing 10 % fetal bovine serum (FBS; Invitrogen). Twenty nanomolar phorbol ester 12-O-tetradecanoyl-phorbol-13-acetate (TPA; Sigma-Aldrich) was used to differentiate U937 cells into macrophages [31,32].

The human NPC cell line CNE-2 was purchased from the Cell Bank of the Shanghai Institute of Biological Science (SIBCB; China) and cultured in Roswell Park Memorial Institute (RPMI)-1640 medium (Gibco) containing 10 % FBS in a 5 % CO₂ incubator at 37 °C. A high-metastatic NPC subclone (HMC) and a low-metastatic NPC subclone (LMC) were screened from the CNE-2 cell line using the limiting dilution method, as previously described [33,34].

To isolate TAMs, NPC tissues were sliced into the smallest possible pieces and digested in DMEM medium containing collagenase (1 mg/mL; Gibco, NY, USA) and DNase I (2 µg/mL; Beyotime, Shanghai, China) at 37 °C for 3 h, then filtered through a 40-µm nylon mesh (Thermo Fisher Scientific, MA, USA). Cell suspensions were stained with a CD68 antibody (eBioscience, CA, USA) for TAM isolation

and analysis.

2.4. Quantitative reverse transcription-polymerase chain reaction (qRT-PCR)

Total RNA was isolated from cells or exosomes with Trizol reagent (Beyotime) in accordance, according to the manufacturer's instructions. Approximately 200 ng of RNA was used to synthesize first-strand cDNA using M-MLV (Thermo Fisher Scientific) and Oligo (dT) primers or miR-193b-specific primers to a final volume of 20 μ L. The temperature protocol for RT-PCR was set as follows: 70 °C for 15 min, ice bath for 2 min, and 42 °C for 60 min. qRT-PCR was performed on a LightCycler 480II real-time PCR system (Roche, Basel, Switzerland) using a Hifair III One-Step qRT-PCR SYBR Green Kit (Yeasen, Shanghai, China). β -actin and U6 were used as internal controls for mRNA and miRNA, respectively. Relative mRNA or miRNA expression levels were calculated using the $2^{-\Delta\Delta Ct}$ method. All primers used are listed in Supporting Table S1.

2.5. Western blot analysis

Total protein was collected using radioimmunoprecipitation assay (RIPA) buffer (Beyotime), and the protein concentration was quantified using a bicinchoninic acid (BCA) protein assay kit (Solarbio, Beijing, China), according to the manufacturer's instructions. Approximately 20 μ g of protein from each sample were separated using 12 % sodium dodecyl-sulfate polyacrylamide gel electrophoresis (SDS-PAGE) and transferred to polyvinylidene fluoride (PVDF) membranes (Roche). Membranes were blocked in 5 % skim milk for 120 min and incubated for 60 min with primary antibodies against CD63 (1:2000, CBL553, Merck, MA, USA), CD9 (1:1000, ab223052, Abcam, CA, USA), CD81 (1:3000, ab109201, Abcam), inducible nitric oxide synthase (iNOS, 1:1000, ab178945, Abcam), CD206 (1:1000, PA5-82136, Thermo Fisher Scientific), MEKK3 (1:1000, A303-133A-T, Thermo Fisher Scientific), and β -actin (1:4000, ab8226, Abcam), followed by incubation with the appropriate second antibodies for 60 min. The bands were visualized using an enhanced chemiluminescence (ECL) kit (Thermo Fisher Scientific) and band density was analyzed using ImageJ software (NIH, USA).

2.6. Transwell assay

Cell migration and invasion were assessed using Transwell chambers (8 μ m, 24-well insert; Corning, NY, USA). For the invasion assay, 30 μ L of diluent Matrigel (Corning) was used to coat the bottom of the Transwell chambers. For the migration assay, the bottom of the Transwell chambers was not covered with Matrigel. Briefly, HMCs or LMCs (1×10^4 /well) cultured in serum-free medium were seeded in the upper chamber and DMEM medium supplemented with 10 % FBS was added to the lower chamber. After 36 h, cells that resided on inner side of Transwell chambers were wiped with a cotton swab, and migrated or invasive cells were fixed with 4 % paraformaldehyde (PFA; Solarbio) for 15 min and stained with 0.1 % crystal violet for 15 min. Finally, the stained cells were photographed using a DM IL LED inverted microscope (Leica, Wetzlar, Germany) and the number of cells that migrated or invaded the lower chamber was counted.

2.7. Exosome isolation

To collect exosomes, HMCs and LMCs (approximately 80 % confluent in 10-cm dishes) were washed with phosphate-buffered saline (PBS), and the complete medium was replaced with exosome-free medium (Gibco) for 48 h. Conditioned medium (CM) was collected to be passed through a 0.22- μ m filter, and exosomes were extracted from the CM through differential ultracentrifugation, as previously described [35,36]. Briefly, the CM was ultracentrifuged at 120,000 \times g for 85 min. The garnered precipitate was dissolved in cold PBS and ultra-centrifuged at 120,000 \times g for 85 min again to collect exosomes, which were resuspended in PBS and stored at -80 °C.

2.8. Identification of exosomes

Exosomes were identified using transmission electron microscopy (TEM), nanoparticle tracking analysis (NTA), and western blotting, as previously described [37]. For TEM, exosomes were fixed in 4 % PFA and placed on copper grids. Exosomes were dyed using 2 % uranyl acetate when the copper grids were dry, then observed at 100 kV. NTA was used to assess the size distribution of exosomes based on the instruction manual of the ZetaView® PMX 110 (Particle Metrix, Meerbusch, Germany). Western blot analysis was performed to assess the exosome-specific markers CD63, CD9, and CD81, as described above.

2.9. miR-193b transferring assay

HMCs (1×10^5 cells/well) were incubated with 20 nM FAM-labeled miR-193b (GenePharma, Shanghai, China) for 24 h and then co-cultured with U937 cells (1×10^5 cells/well) in Transwell chambers (Corning). The fluorescence signal in the HMCs and U937 cells was assessed using a TCS-STED confocal microscope (Leica) after co-culturing for 36 h.

2.10. Nitric oxide (NO) and lactate production

U937 cells were treated with HMC-Exos, HMC-Exos + GW4869 (an inhibitor of exosome biogenesis/release), miR-193b, and IL-4 or IFN- γ + lipopolysaccharide (LPS) as a control. The cell culture supernatant was collected to assess NO (ab65328, Abcam) and lactate

(ab65330, Abcam) levels, according to the manufacturer’s instructions.

2.11. Luciferase reporter assay

The speculative miR-193b complementary sequence in the *MEKK3* 3'-untranslated region (UTR) was amplified using PCR and cloned into the pGL3 vector to construct a recombinant plasmid of the pGL3-MEKK3-3'UTR-Wt. pGL3-MEKK3-3'UTR-Mut plasmid was constructed using a site-directed mutagenesis kit (Sangon Biotech). For the luciferase reporter assay, CNE-2 cells (1×10^5 cells/well), seeded into 48-well plates, were co-transfected with 40 nM of miR-193b, 15 ng of either pGL3-MEKK3-3'UTR-Wt or pGL3-MEKK3-3'UTR-Mut, and 1.5 ng of pRL-TK (Promega, Madison, WI) using Lipofectamine 3000 (Invitrogen). After incubation for 48 h, the cells were collected to assess relative luciferase activity using the Dual-Luciferase Reporter Assay System (Promega), according to the manufacturer’s instructions.

2.12. Clonogenic survival assay

CM was collected from miR-193b-overexpressed U937 cells and used to treat LMCs. Under these conditions, LMCs received different doses of irradiation (0, 2, 4, 8, and 10 Gy) for 2 weeks, and colonies exceeding 50 cells were counted to calculate the surviving fractions, as previously described [38–40].

2.13. Statistics

The data are shown as the mean \pm standard deviation (S.D.) from three independent experiments. Differences were assessed using Student’s *t*-test (two groups) or analysis of variance (ANOVA) followed by the Scheffé test (multiple groups) using GraphPad Prism 7.0 (CA, USA). Statistical significance was set at $p < 0.05$.

3. Results

3.1. HMC-Exos facilitated TAM activation

To investigate the correlation between macrophage phenotype and NPC metastasis, HMCs and LMCs were screened from the CNE-2 cell line as previously described [34,41]. The results of the Transwell invasion assay showed that HMCs exhibited higher invasive activity than LMCs (Fig. 1A). The roles of HMCs and LMCs in the regulation of macrophage phenotypes were explored by assessing the expression of inflammatory- and immunosuppression-related genes. Fig. 1B shows that macrophages co-cultured with HMCs displayed generally increased expression of immunosuppression-related genes compared to macrophages co-cultured with LMCs, accompanied

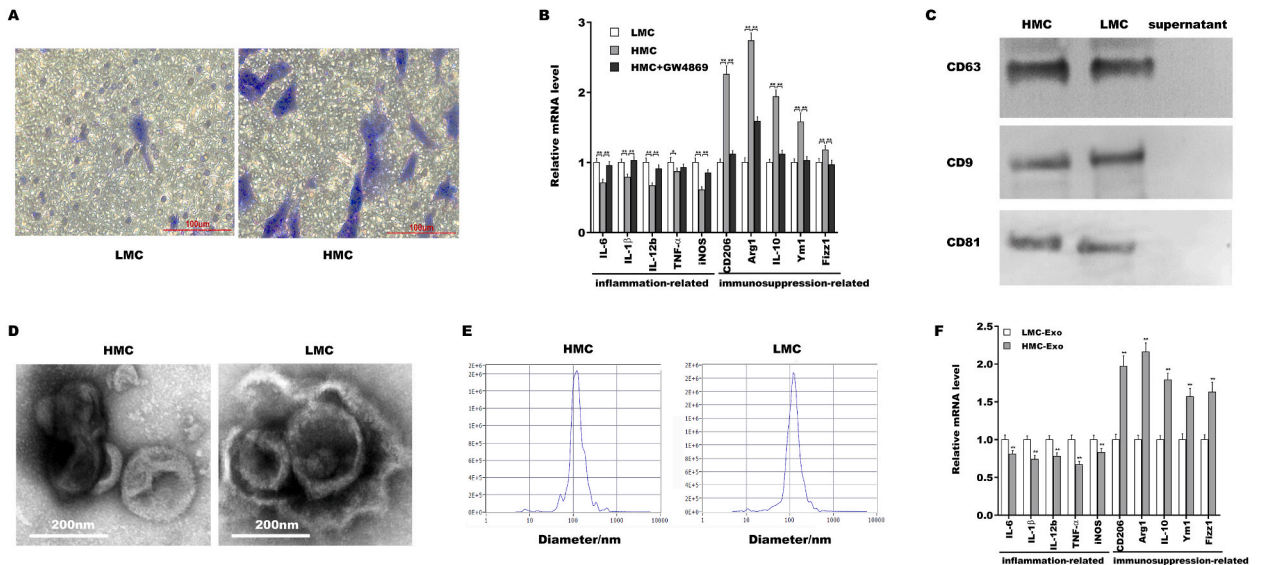


Fig. 1. HMC-Exos facilitated TAM activation. (A) HMCs and LMCs were screened from the CNE-2 cell line using the limiting dilution method, then a Transwell invasion assay was performed to assess HMC and LMC invasive capacity. Scale bar = 100 μ m. (B) After treatment with 20 nM TPA for 48 h, U937 cells were co-cultured with LMCs, HMCs, and GW4869-treated HMCs. Next, qRT-PCR was performed to assess the expression level of inflammation- and immunosuppression-related genes. Exosomes were identified using Western blot analysis for CD63, CD9, and CD81 (C), TEM (D), and NTA (E). (F) After treatment with 20 nM TPA for 48 h, U937 cells were treated with LMC-Exos or HMC-Exos, then qRT-PCR was performed to assess the expression level of inflammation- and immunosuppression-related genes. $*p < 0.01$.

by decreased expression of inflammation-related genes. These data indicate that HMCs polarize macrophages toward an immunosuppressive phenotype (that is, TAM activation). GW4869 treatment disrupts the effects of HMCs on TAM activation. Because of the crucial role of exosomes in intercellular communication between NPC cells and macrophages, exosomes were collected from the conditioned medium of HMCs and LMCs and characterized using western blotting, TEM, and qNano analyses. Western blot analysis revealed that the collected products expressed exosomal markers (CD63, CD9, and CD81) (Fig. 1C). TEM analysis revealed that the collected products had a characteristic cup-like shape (Fig. 1D). qNano analysis showed that these products were microvesicles with diameters of 80–130 nm (Fig. 1E). Fig. 1F shows a generally increased expression of immunosuppression-related genes, accompanied by a decreased expression of inflammation-related genes, in HMC-Exo-treated macrophages compared to LMC-Exo treatment. These results suggest that HMC-Exos facilitate TAM activation.

3.2. miR-193b was upregulated in HMC-Exos and metastatic NPC tissues-derived TAMs

Exosomal miRNAs play important roles in mediating the intercellular communication between cancer cells and macrophages [42, 43]. To identify functional miRNAs in NPC cell-derived exosomes, two datasets (GSE48502 and GSE118720) were downloaded from the GEO database. Venn diagram analysis revealed that two miRNAs (miR-196a and miR-193b) were concurrently upregulated in metastatic and radioresistant NPC tissues in both datasets (Fig. 2A, Supporting Table S2). The expression levels of miR-196a and miR-193b were higher in HMCs than in LMCs (Fig. 2B), and only miR-193b expression was significantly higher in HMC-Exos than in LMC-Exos (Fig. 2C). Interestingly, miR-193b was broadly expressed in the macrophages of NPC tissues (Fig. 2D). We further demonstrated that miR-193b levels were higher in TAMs than in BDMs (Fig. 2E) and that miR-193b was increased in metastatic NPC tissue-derived TAMs compared to non-metastatic NPC tissue-derived TAMs (Fig. 2F). These results suggest that NPC cell-derived exosomal miR-193b may be transferred to TAMs to promote tumor metastasis.

3.3. miR-193b was transferred to macrophages from HMCs through exosomes

To explore whether miR-193b could be transferred to macrophages from HMC-Exos, miR-193b was overexpressed in HMCs, and its level was assessed in HMCs and HMC-Exos. Fig. 3A and B shows that miR-193b expression was significantly elevated in HMCs and HMC-Exos after miR-193b mimic transfection, indicating that miR-193b can be packaged into exosomes in HMCs. Treatment with miR-193b-overexpressed HMCs-derived exosomes upregulated miR-193b expression in the recipient U937 cells (Fig. 3C), suggesting that exosomal miR-193b can be transferred to macrophages. To further assess the miR-193b transfer from HMCs to macrophages, HMCs were treated with FAM-labeled miR-193b (Fig. 3D) and co-cultured with U937 cells. Fig. 3E shows that FAM-labeled miR-193b was detected in U937 cells, suggesting that miR-193b can be transferred from HMCs to macrophages through exosomes.

3.4. miR-193b facilitated TAM activation by repressing MEKK3

Next, the function of miR-193b in regulating macrophage phenotype (or TAM activation) was investigated. Fig. 4A shows the

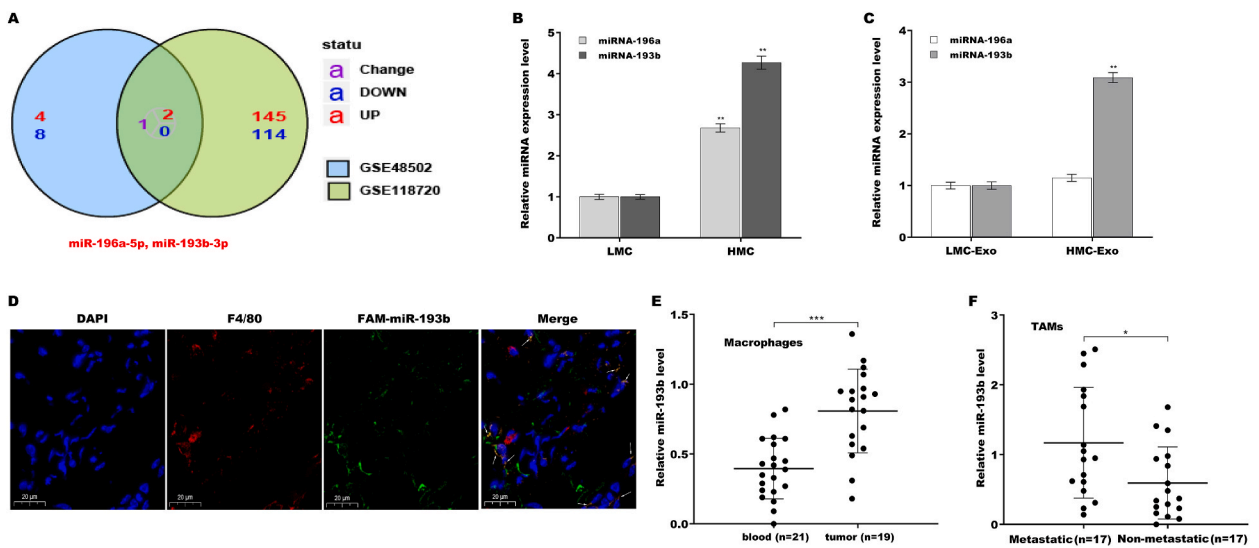


Fig. 2. miR-193b was up-regulated in HMC-Exos and metastatic NPC tissue-derived TAMs. (A) GSE48502 and GSE118720 were downloaded from the GEO database, and Venn diagram analysis was performed to identify differentially expressed miRNAs in both sets of data. qRT-PCR analysis was performed to assess miR-196a and miR-193b expression levels in HMCs and LMCs (B), and in HMC-Exos and LMC-Exos (C). (D) Representative IF images show F4/80 and miR-193b expression in NPC tissues. (E) qRT-PCR analysis of miR-193b levels in BDMs (n = 21) and TAMs (n = 19). (F) qRT-PCR analysis of miR-193b levels in TAMs isolated from metastatic (n = 17) and non-metastatic (n = 17) NPC tissues. **p < 0.01.

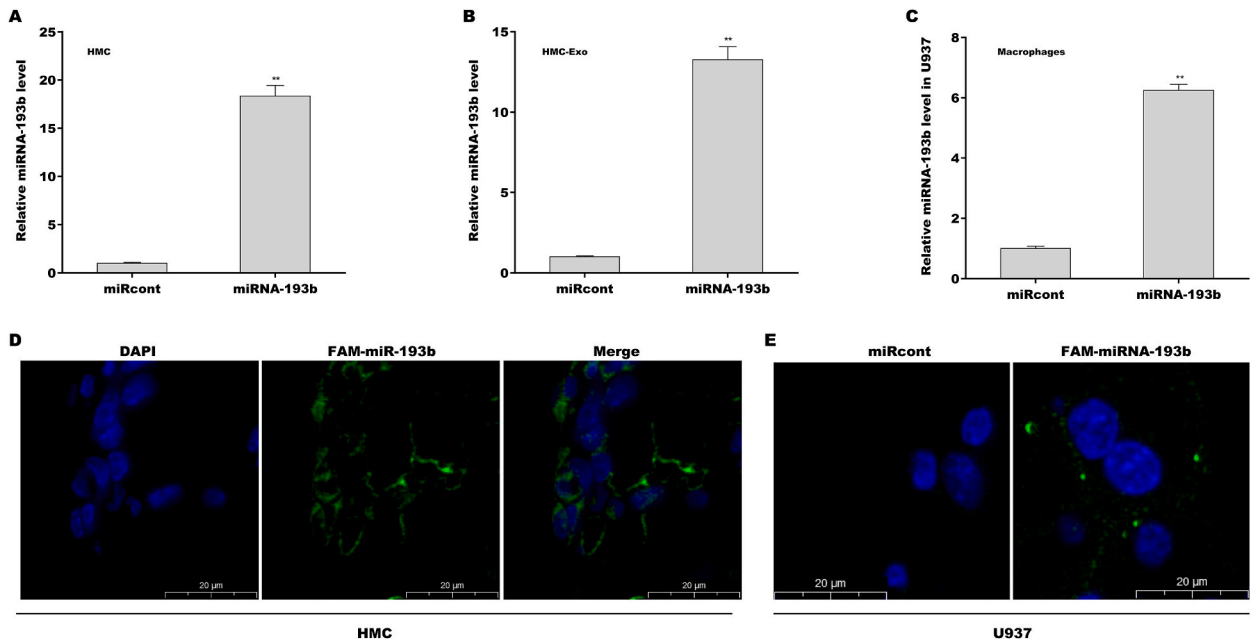


Fig. 3. miR-193b was transferred to macrophages from HMC through exosomes. qRT-PCR analysis of miR-193b levels in HMCs (A), HMC-Exos (B), and U937 cells treated with miR-193b-overexpressed HMC-derived exosomes (C). (D) HMCs were treated with FAM-labeled miR-193b, and fluorescence signals were assessed. (E) HMCs were treated with FAM-labeled miR-193b and co-cultured with TPA-treated U937 cells. Fluorescence signals were assessed in U937 cells. $**p < 0.01$.

generally increased expression of immunosuppression-related genes in miR-193b-treated macrophages compared to those exposed to miRcont treatment (Supporting Fig. S1), indicating that miR-193b facilitated TAM activation. Western blot analysis revealed that miR-193b overexpression increased CD206 and Arg-1 protein expression and decreased iNOS protein expression (Fig. 4B and C). The production of NO and lactate, indicators of inflammatory and immunosuppressive macrophage activation, were assessed to further evaluate the role of miR-193b in TAM activation. Fig. 4D and E shows that miR-193b decreased NO levels and increased lactate production. These data further verify the role of HMC-Exos in TAM activation (Fig. 4D and E).

To identify the target genes of miR-193b, the TargetScan tool (<http://www.targetscan.org/>) was used to predict the potential target genes of miR-193b (Supporting Table S3). Additionally, the GSE118720 dataset was used to analyze the differentially expressed mRNAs (Supporting Table S4). Venn diagram analysis revealed 53 common mRNAs between these two sets of data (Fig. 4F, Supporting Table S5). Of these genes, the *MEKK3* was selected for subsequent validation because it is known to be involved in the macrophage phenotype [44,45]. Sequence analysis revealed a binding site for miR-193b in *MEKK3*-3'UTR (Fig. 4G). To verify the regulatory role of miR-193b in *MEKK3* expression by targeting *MEKK3*-3'UTR, pGL3-*MEKK3*-3'UTR-wt recombinant plasmid or its mutant (pGL3-*MEKK3*-3'UTR-mut) was constructed and transfected into U937 cells with miR-193b. The results from the dual luciferase reporter gene assay revealed that miR-193b significantly inhibited pGL3-*MEKK3*-3'UTR-wt luciferase activity, whereas miR-193b did not affect pGL3-*MEKK3*-3'UTR-mut luciferase activity (Fig. 4H). Furthermore, although miR-193b did not alter *MEKK3* mRNA levels (data not shown), miR-193b significantly reduced *MEKK3* protein expression (Fig. 4I). These results demonstrate that miR-193b facilitates TAM activation by regulating *MEKK3* expression.

3.5. miR-193b-overexpressed macrophages facilitated NPC cell invasion and radioresistance

Finally, the role of miR-193b-induced TAM activation in the regulation of NPC cell invasion and radioresistance was assessed. U937 cells were treated with miR-193b mimics, and the CM was collected to treat LMCs. Fig. 5A and B shows that CM derived from miR-193b-overexpressed macrophages significantly accelerated LMC migration. The CM derived from miR-193b-overexpressed macrophages also facilitated LMC invasion (Fig. 5C and D). Moreover, miR-193b delivery resulted in significant radioresistance in LMCs compared to miRcont delivery (Fig. 5E and F).

4. Discussion

Macrophages are a major type of immune cell in the TME, and immunosuppressive TAMs commonly aggregate in the TME to accelerate angiogenesis and matrix remodeling and produce growth factors, promoting cancer cell growth, invasion, and radioresistance [46]. Expanding evidence has demonstrated that the direct interaction of cancer cells with macrophages is a critical factor in the development of an immunosuppressive TME [14,46]. In the present study, we demonstrated that: i) HMC-Exos promote TAM

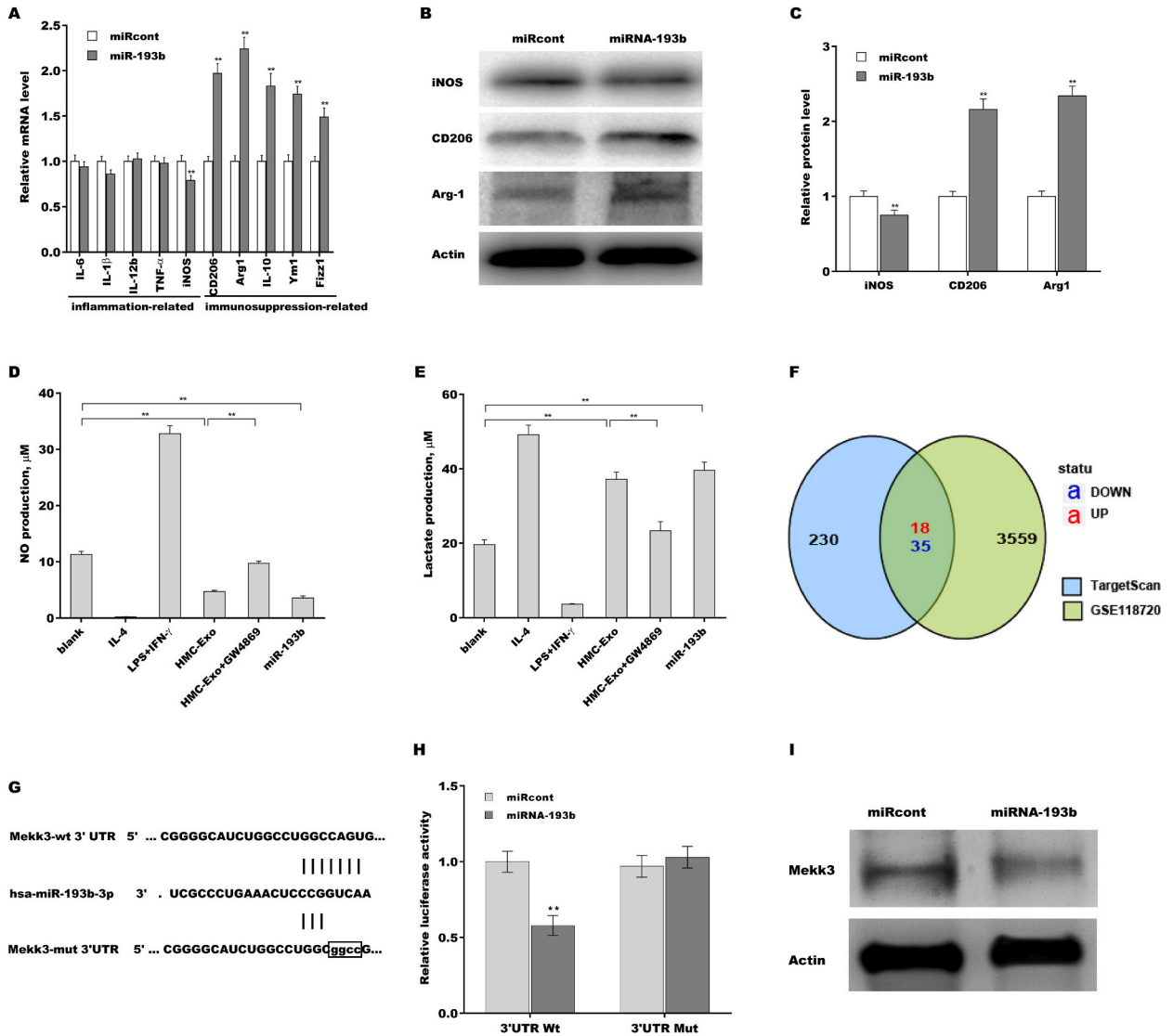


Fig. 4. miR-193b facilitated TAM activation by repressing MEKK3. U937 cells were treated with 20 nM TPA for 48 h, then the following experiments were performed: (A) U937 cells were treated with miR-193b mimics, and qRT-PCR was performed to assess the expression levels of inflammation- and immunosuppression-related genes. Western blot (B) and quantitative (C) analyses of iNOS, CD206, and Arg-1 expression in U937 cells after miR-193b overexpression. U937 cells were treated with the indicated reagents, and NO (D) and lactate (E) production was assessed using the indicated assay kit. (F) The TargetScan tool was used to predict the potential target genes of miR-193b. The GSE118720 dataset was used to analyze differentially expressed mRNAs. Venn diagram analysis was performed to identify the common genes between these two datasets. (G) Schematic diagram of the speculative miR-193b complementary sequence in the *MEKK3* 3'-UTR. (H) A luciferase reporter assay was performed using CNE-2 cells after co-transfection with miR-193b, pGL3-MEKK3-3'-UTR-Wt, or pGL3-MEKK3-3'-UTR-Mut. (I) Western blot analysis of MEKK3 expression in miR-193b-overexpressed CNE-2 cells. ****p < 0.01.**

activation, ii) miR-193b is increased in HMC-Exos and metastatic NPC tissue-derived TAMs, iii) HMC-derived exosomal miR-193b can be transferred to macrophages, iv) miR-193b accelerates TAM activation by repressing MEKK3, and v) miR-193b-overexpressed macrophages promote NPC cell invasion and radioresistance. These results, together with those of previous studies, indicate that TAMs may be the center of the immunosuppressive TME and a potential target for the treatment of human tumors.

Macrophages are heterogeneous in the TME, depending on the tumor type, grade, and location within the tumor lesion [47]. Although the M1/M2 phenotype has been defined in previous studies [48–50], excessive M1/M2 polarization cannot objectively describe macrophage stage and function, and the M1/M2 nomenclature has been mostly discarded [51]. In the TME, the macrophage phenotype is influenced by the different types of cells surrounding it, including tumor cells and cancer-associated fibroblasts (CAFs) [14,52,53]. Zhao et al. reported that CAFs contribute to TAM activation by exosomal miR-320a-regulated PTEN/PI3K γ signaling [54]. In this study, we demonstrated that NPC cell-derived exosomes promote macrophage pro-tumorigenic activation (that is, TAM

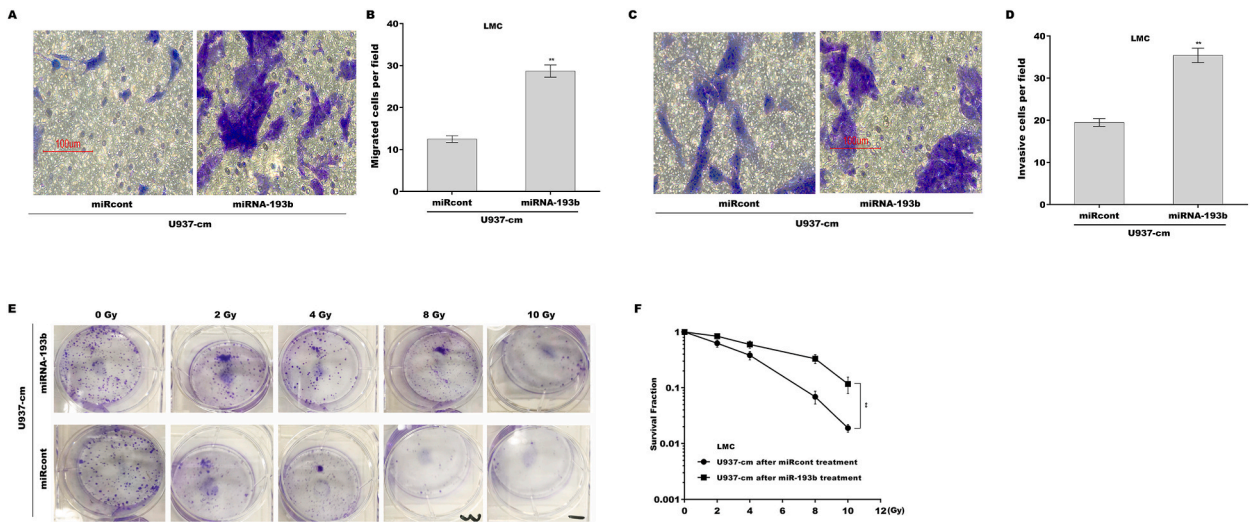


Fig. 5. miR-193b-overexpressed macrophages facilitated NPC cell invasion and radioresistance. After treatment with 20 nM TPA for 48 h, U937 cells were treated with miR-193b mimics or miRNA controls, and the CM was collected to treat the LMCs. Transwell migration assays (A) and quantitative analyses (B) were performed to assess the migration capacity of LMCs. Scale bar = 100 µm. Transwell invasion assays (C) and quantitative analyses (D) were performed to assess the invasive capacity of LMCs. (E and F) A clonogenic survival assay was performed to assess the role of CM derived from miR-193b-overexpressed macrophages in regulating radioresistance. ***p* < 0.01.

activation), as evidenced by the generally increased expression of immunosuppression-related genes and decreased expression of inflammation-related genes. In addition to exosomes, intercellular interactions between cancer cells and macrophages are mediated in other ways. Wang et al. demonstrated that cancer cells accelerate TAM activation by increasing lysosome-associated membrane protein type 2A (LAMP2a) expression in macrophages, and higher LAMP2a levels in TAMs predict more negative clinical outcomes in patients with breast cancer [14]. Understanding the communication mechanism between different cells in the TME is essential.

miRNAs play a vital role in exosome-mediated cell-cell communication in the TME, that is, intercellular communication between cancer cells and CAFs. HCC-derived exosomal miR-1247-3p facilitates CAF activation to promote cancer metastasis by regulating NF-κB signaling [20]. Intrahepatic cholangiocarcinoma (ICC) cell-derived exosomal miR-183-5p facilitates macrophage pro-tumorigenic activation by regulating the phosphatase and tensin homolog (PTEN)/AKT/PD-L 1 axis [42]. In contrast, the “M2” macrophage-derived exosomal miRNA-21-5p accelerates renal cell carcinoma (RCC) progression by regulating the PTEN/AKT pathway [55]. The current results show that highly metastatic NPC cell-derived exosomal miR-193b-3p activates TAM, resulting in cancer cell invasion and radioresistance.

The biological role of miR-193b in the regulation of cancer cell proliferation and inflammatory responses remains controversial. miR-193b is an oncomiRNA in colorectal cancer (CRC) [56]. miR-193b overexpression accelerates CRC cell proliferation by repressing methyltransferase SUV39H1 expression [56]. In T-cell acute lymphoblastic leukemia (T-ALL), miR-193b acts as a tumor suppressive gene [57]. miR-193b inhibition contributes to cancer cell proliferation by de-repressing notch receptor 1 (NOTCH1) [57]. In keratinocytes, miR-193b represses cell proliferation and the production of inflammatory cytokines by regulating STAT3 and NF-κB signaling [58]. A recent study showed that miR-193b expression levels are dysregulated during macrophage polarization [59], indicating a potential role of miR-193b in macrophage polarization. However, their role in TEM remains unclear. In the present study, we demonstrated that HMC-Exos contain a high abundance of miR-193b and that exosomal miR-193b can be transferred to macrophages to promote macrophage pro-tumorigenic activation by suppressing MEKK3 expression. Consequently, miR-193b-overexpressed macrophages facilitate NPC cell invasion and radioresistance. The study had the following three major limitations: i) in the studies of assessing miR-193b levels in BDMs, TAMs, and NPC tissues (Fig. 2), the sample size was not sufficiently large. It is necessary to assess miR-193b levels in a larger sample size; ii) it would be meaningful to measure miR-193b levels in the peripheral blood of patients with NPC at different stages to evaluate its feasibility as a serum biomarker; and iii) It is necessary to further confirm the roles of miR-193b in regulating TAM activation and NPC radioresistance using mouse subcutaneous tumor model.

5. Conclusions

These results demonstrate that NPC cell-derived exosomal miR-193b-3p activates TAMs and results in cancer cell invasion and radioresistance, which revealed a critical role of exosomal miR-193b-3p in mediating intercellular communication between NPC cells and macrophages, providing a potential target for NPC treatment.

Ethics approval

This work was approved by the Ethics Committee of the Fudan University Shanghai Cancer Center (NO. 050432-2108*).

Funding statement

No funding.

Data availability statement

All relevant data supporting the conclusions of this article is included within this manuscript.

CRedit authorship contribution statement

Weiwei Li: Writing – original draft, Formal analysis, Data curation, Conceptualization. **Xing Xing:** Project administration, Methodology, Investigation, Funding acquisition, Data curation, Conceptualization. **Chunying Shen:** Software, Resources, Project administration, Methodology, Investigation. **Chaosu Hu:** Writing – review & editing, Writing – original draft, Funding acquisition, Formal analysis, Data curation, Conceptualization.

Declaration of competing interest

The authors declare that they have no known competing financial interests or personal relationships that could have appeared to influence the work reported in this paper.

Appendix A. Supplementary data

Supplementary data to this article can be found online at <https://doi.org/10.1016/j.heliyon.2024.e30808>.

References

- [1] B. Brennan, Nasopharyngeal carcinoma, *Orphanet J. Rare Dis.* 1 (2006) 23.
- [2] H. Sung, et al., Global cancer statistics 2020: GLOBOCAN estimates of incidence and mortality worldwide for 36 cancers in 185 countries, *CA A Cancer J. Clin.* 71 (3) (2021) 209–249.
- [3] Y.P. Chen, et al., Nasopharyngeal carcinoma, *Lancet* 394 (10192) (2019) 64–80.
- [4] Y. Lin, et al., Protein tyrosine phosphatase receptor type D gene promotes radiosensitivity via STAT3 dephosphorylation in nasopharyngeal carcinoma, *Oncogene* 40 (17) (2021) 3101–3117.
- [5] P. Blanchard, et al., Chemotherapy and radiotherapy in nasopharyngeal carcinoma: an update of the MAC-NPC meta-analysis, *Lancet Oncol.* 16 (6) (2015) 645–655.
- [6] Y.P. Chen, et al., A Bayesian network meta-analysis comparing concurrent chemoradiotherapy followed by adjuvant chemotherapy, concurrent chemoradiotherapy alone and radiotherapy alone in patients with locoregionally advanced nasopharyngeal carcinoma, *Ann. Oncol.* 26 (1) (2015) 205–211.
- [7] T. Hagemann, et al., "Re-educating" tumor-associated macrophages by targeting NF-kappaB, *J. Exp. Med.* 205 (6) (2008) 1261–1268.
- [8] M. Chittiezath, et al., Molecular profiling reveals a tumor-promoting phenotype of monocytes and macrophages in human cancer progression, *Immunity* 41 (5) (2014) 815–829.
- [9] K. Arvanitakis, et al., Tumor-associated macrophages in hepatocellular carcinoma pathogenesis, prognosis and therapy, *Cancers* 14 (1) (2022).
- [10] M. Yang, et al., Diverse functions of macrophages in different tumor microenvironments, *Cancer Res.* 78 (19) (2018) 5492–5503.
- [11] N. Graham, J.W. Pollard, An acid trip activates protumoral macrophages to promote hepatocellular carcinoma malignancy, *J. Clin. Invest.* 132 (7) (2022).
- [12] E. Guc, J.W. Pollard, Redefining macrophage and neutrophil biology in the metastatic cascade, *Immunity* 54 (5) (2021) 885–902.
- [13] R. Noy, J.W. Pollard, Tumor-associated macrophages: from mechanisms to therapy, *Immunity* 41 (1) (2014) 49–61.
- [14] R. Wang, et al., Tumor cells induce LAMP2a expression in tumor-associated macrophage for cancer progression, *EBioMedicine* 40 (2019) 118–134.
- [15] A. Mantovani, et al., Tumour-associated macrophages as treatment targets in oncology, *Nat. Rev. Clin. Oncol.* 14 (7) (2017) 399–416.
- [16] P.S. Yang, et al., Targeting protumor factor chitinase-3-like-1 secreted by Rab37 vesicles for cancer immunotherapy, *Theranostics* 12 (1) (2022) 340–361.
- [17] M. Zhou, et al., Exosome derived from tumor-associated macrophages: biogenesis, functions, and therapeutic implications in human cancers, *Biomark. Res.* 11 (1) (2023) 100.
- [18] X. Wang, et al., Hypoxic tumor-derived exosomal miR-301a mediates M2 macrophage polarization via PTEN/PI3Kgamma to promote pancreatic cancer metastasis, *Cancer Res.* 78 (16) (2018) 4586–4598.
- [19] J. Xun, et al., Cancer-derived exosomal miR-138-5p modulates polarization of tumor-associated macrophages through inhibition of KDM6B, *Theranostics* 11 (14) (2021) 6847–6859.
- [20] T. Fang, et al., Tumor-derived exosomal miR-1247-3p induces cancer-associated fibroblast activation to foster lung metastasis of liver cancer, *Nat. Commun.* 9 (1) (2018) 191.
- [21] L. Milane, et al., Exosome mediated communication within the tumor microenvironment, *J. Contr. Release* 219 (2015) 278–294.
- [22] R. Li, et al., Exosomes from adipose-derived stem cells regulate M1/M2 macrophage phenotypic polarization to promote bone healing via miR-451a/MIF, *Stem Cell Res. Ther.* 13 (1) (2022) 149.
- [23] M. Wang, B. Zhang, The immunomodulation potential of exosomes in tumor microenvironment, *J Immunol Res* 2021 (2021) 3710372.
- [24] P.J. Lee, et al., Epstein-Barr viral product-containing exosomes promote fibrosis and nasopharyngeal carcinoma progression through activation of YAP1/FAPalpha signaling in fibroblasts, *J. Exp. Clin. Cancer Res.* 41 (1) (2022) 254.
- [25] F.Z. Wan, et al., Exosomes overexpressing miR-34c inhibit malignant behavior and reverse the radioresistance of nasopharyngeal carcinoma, *J. Transl. Med.* 18 (1) (2020) 12.

- [26] J. Jiang, et al., Radiosensitizer EXO-miR-197-3p inhibits nasopharyngeal carcinoma progression and radioresistance by regulating the AKT/mTOR Axis and HSPA5-mediated autophagy, *Int. J. Biol. Sci.* 18 (5) (2022) 1878–1895.
- [27] C.W. Li, et al., Exosomal miR-106a-5p accelerates the progression of nasopharyngeal carcinoma through FBXW7-mediated TRIM24 degradation, *Cancer Sci.* 113 (5) (2022) 1652–1668.
- [28] J. Li, et al., Exosomal transfer of miR-106a-5p contributes to cisplatin resistance and tumorigenesis in nasopharyngeal carcinoma, *J. Cell Mol. Med.* 25 (19) (2021) 9183–9198.
- [29] M. Jinushi, et al., Tumor-associated macrophages regulate tumorigenicity and anticancer drug responses of cancer stem/initiating cells, *Proc. Natl. Acad. Sci. U. S. A.* 108 (30) (2011) 12425–12430.
- [30] M. Lasch, et al., Isolation of decidual macrophages and Hofbauer cells from term placenta-comparison of the expression of CD163 and CD80, *Int. J. Mol. Sci.* 23 (11) (2022).
- [31] J. Savikko, et al., Epidermal growth factor receptor inhibition by erlotinib prevents vascular smooth muscle cell and monocyte-macrophage function in vitro, *Transpl. Immunol.* 32 (3) (2015) 175–178.
- [32] S. Cathelin, et al., Identification of proteins cleaved downstream of caspase activation in monocytes undergoing macrophage differentiation, *J. Biol. Chem.* 281 (26) (2006) 17779–17788.
- [33] Y.Y. Liang, et al., Downregulation of Ras association domain family member 6 (RASSF6) underlies the treatment resistance of highly metastatic nasopharyngeal carcinoma cells, *PLoS One* 9 (7) (2014) e100843.
- [34] C.N. Qian, et al., Preparing the "soil": the primary tumor induces vasculature reorganization in the sentinel lymph node before the arrival of metastatic cancer cells, *Cancer Res.* 66 (21) (2006) 10365–10376.
- [35] J. Hu, et al., Exosomal miR-17-5p from adipose-derived mesenchymal stem cells inhibits abdominal aortic aneurysm by suppressing TXNIP-NLRP3 inflammasome, *Stem Cell Res. Ther.* 13 (1) (2022) 349.
- [36] J.L. Hu, et al., CAFs secreted exosomes promote metastasis and chemotherapy resistance by enhancing cell stemness and epithelial-mesenchymal transition in colorectal cancer, *Mol. Cancer* 18 (1) (2019) 91.
- [37] H. Xing, et al., Injectable exosome-functionalized extracellular matrix hydrogel for metabolism balance and pyroptosis regulation in intervertebral disc degeneration, *J. Nanobiotechnol.* 19 (1) (2021) 264.
- [38] S. Xu, et al., LZTS2 inhibits PI3K/AKT activation and radioresistance in nasopharyngeal carcinoma by interacting with p85, *Cancer Lett.* 420 (2018) 38–48.
- [39] X.P. Feng, et al., Identification of biomarkers for predicting nasopharyngeal carcinoma response to radiotherapy by proteomics, *Cancer Res.* 70 (9) (2010) 3450–3462.
- [40] W. Huang, et al., Cancer-associated fibroblasts promote the survival of irradiated nasopharyngeal carcinoma cells via the NF-kappaB pathway, *J. Exp. Clin. Cancer Res.* 40 (1) (2021) 87.
- [41] X. Hong, et al., Circular RNA CRIM1 functions as a ceRNA to promote nasopharyngeal carcinoma metastasis and docetaxel chemoresistance through upregulating FOXQ1, *Mol. Cancer* 19 (1) (2020) 33.
- [42] C. Luo, et al., Tumor-derived exosomes induce immunosuppressive macrophages to foster intrahepatic cholangiocarcinoma progression, *Hepatology* (2022).
- [43] Z. Xu, et al., Role of exosomal non-coding RNAs from tumor cells and tumor-associated macrophages in the tumor microenvironment, *Mol. Ther.* (2022).
- [44] H. Fang, et al., MiR-132-3p modulates MEKK3-dependent NF-kappaB and p38/JNK signaling pathways to alleviate spinal cord ischemia-reperfusion injury by hindering M1 polarization of macrophages, *Front. Cell Dev. Biol.* 9 (2021) 570451.
- [45] K. Kim, et al., MEKK3 is essential for lipopolysaccharide-induced interleukin-6 and granulocyte-macrophage colony-stimulating factor production in macrophages, *Immunology* 120 (2) (2007) 242–250.
- [46] J. Condeelis, J.W. Pollard, Macrophages: obligate partners for tumor cell migration, invasion, and metastasis, *Cell* 124 (2) (2006) 263–266.
- [47] D.I. Gabrilovich, S. Ostrand-Rosenberg, V. Bronte, Coordinated regulation of myeloid cells by tumours, *Nat. Rev. Immunol.* 12 (4) (2012) 253–268.
- [48] D. Date, et al., Kruppel-like transcription factor 6 regulates inflammatory macrophage polarization, *J. Biol. Chem.* 289 (15) (2014) 10318–10329.
- [49] H. Huang, et al., M2-polarized tumour-associated macrophages in stroma correlate with poor prognosis and Epstein-Barr viral infection in nasopharyngeal carcinoma, *Acta Otolaryngol.* 137 (8) (2017) 888–894.
- [50] J. Wang, et al., Tumor cells induced-M2 macrophage favors accumulation of Treg in nasopharyngeal carcinoma, *Int. J. Clin. Exp. Pathol.* 10 (8) (2017) 8389–8401.
- [51] P.J. Murray, et al., Macrophage activation and polarization: nomenclature and experimental guidelines, *Immunity* 41 (1) (2014) 14–20.
- [52] M. Zhang, et al., Pancreatic cancer cells render tumor-associated macrophages metabolically reprogrammed by a GARP and DNA methylation-mediated mechanism, *Signal Transduct. Targeted Ther.* 6 (1) (2021) 366.
- [53] X. Mao, et al., Crosstalk between cancer-associated fibroblasts and immune cells in the tumor microenvironment: new findings and future perspectives, *Mol. Cancer* 20 (1) (2021) 131.
- [54] M. Zhao, A. Zhuang, Y. Fang, Cancer-associated fibroblast-derived exosomal miRNA-320a promotes macrophage M2 polarization in vitro by regulating PTEN/PI3Kgamma signaling in pancreatic cancer, *JAMA Oncol.* 2022 (2022) 9514697.
- [55] Z. Zhang, et al., The miRNA-21-5p payload in exosomes from M2 macrophages drives tumor cell aggression via PTEN/Akt signaling in renal cell carcinoma, *Int. J. Mol. Sci.* 23 (6) (2022).
- [56] R. Dinami, et al., TRF2 cooperates with CTCF for controlling the oncomiR-193b-3p in colorectal cancer, *Cancer Lett.* 533 (2022) 215607.
- [57] H. Feng, F. Li, P. Tang, Circ_0000745 regulates NOTCH1-mediated cell proliferation and apoptosis in pediatric T-cell acute lymphoblastic leukemia through adsorbing miR-193b-3p, *Hematology* 26 (1) (2021) 885–895.
- [58] C. Huang, et al., Correction: MiR-193b-3p-ERBB4 axis regulates psoriasis pathogenesis via modulating cellular proliferation and inflammatory-mediator production of keratinocytes, *Cell Death Dis.* 12 (11) (2021) 1072.
- [59] J.W. Graff, et al., Identifying functional microRNAs in macrophages with polarized phenotypes, *J. Biol. Chem.* 287 (26) (2012) 21816–21825.